CSCE Annual Conference

Growing with youth – Croître avec les jeunes

Laval (Greater Montreal)

June 12 - 15, 2019

ASSESSING THE SEISMIC COLLAPSE SAFETY OF CONCRETE BEAM COLUMN JOINTS REINFORCED WITH DIFFERENT SHAPE MEMORY ALLOY REBARS

Mumtasirun Nahar[1], AHM Muntasir Billah[2]
[1]Department of Civil Engineering, Military Institute of Science and Technology, Dhaka, Bangladesh
[2]Department of Civil Engineering, Lakehead University, Thunder Bay, ON, Canada

Abstract: In recent years, shape memory alloy (SMA) have drawn significant attention and interests among researchers and structural engineers for diverse civil engineering applications. Superelasticity, shape memory effect, and hysteretic damping, are the three major attributes of SMAs that make them ideally suited for applications in concrete frames. Among different compositions of SMA, Nickel-Titanium (NiTi) SMA has gained much attention for its superior mechanical and thermal performance over other compositions. However, the high cost and low machinability restricts the widespread use of NiTi SMAs in structural applications. Recently, several compositions of SMAs have been developed, such as Fe-based and Cu-based SMAs, which offer significantly lower cost and superior machinability compared to commonly used NiTi SMAs. The objective of this study is to evaluate the comparative seismic collapse safety of concrete beam-column joints reinforced with five different SMAs. The beam-column joint is assumed to be part of a seven storey moment resistant frame building located in Dhaka, Bangladesh. A total of 20 near fault and far field ground motions will be considered for developing the collapse fragility curves. The collapse safety of the five different SMA-RC beam-column joints will be evaluated interms of maximum inter-storey drift as the demand parameter as well as through development of collapse margin ratios.

Keywords: Seismic fragility, Shape memory alloy, Maximum Drift, Collapse margin ratio.

1 INTRODUCTION

Behavior of reinforced concrete structure is strongly dependent on the interaction between the concrete and the steel reinforcement. Beam-column joint in reinforced concrete structure is one of the critical points for the proper transmission of forces in the structure. However, previous history of earthquake indicates that deficient design of a beam-column joint can jeopardize the integrity of entire structure. Most of the structural collapse that occurred during the earthquakes around the world (1994 Northridge; 1989 Loma Prieta) shows most costly natural disasters in a country‘s economy (Clark et al. 1995). The earthquakes caused unpredictable damage and disruption to the structure as well as posed a great threat to human lives. During the 1995 Hyogo-Ken Nanbu earthquake (Kobe, Japan), more than 100 reinforced concrete (RC) bridge piers experienced more than 1° (1.75%) of permanent deformation, which compelled the government to demolish and rebuild the structures as it was hard to straighten them (Ramirez et al. 2012). One of the most recent devastating earthquakes occurred on April 2015 in Nepal, where the earthquake with a magnitude of 7.8 killed nearly 9000 people and injured nearly 22, 000 people (USGS). This earthquake event has raised many questions regarding the adequacy of current seismic code provisions. Recognizing the extreme vulnerability of reinforced concrete buildings against seismic load, design codes

provide stricter seismic provisions for the detailing of building components against dynamic load. In conventional design of a RC structure earthquake energy is dissipated through yielding of reinforcement and causes permanent deformation of the structure. If Shape Memory alloy (SMA) is used as reinforcements instead of steel in the desired locations of beams, it will not only be able to dissipate adequate seismic energy, but will also be able to restore its original shape after the seismic event by heating (through shape memory effect) or simply upon stress removal (through superelasticity). In this study the performance of reinforced concrete beam-column joint has been assessed using five different types of SMA in terms of Collapse Margin Ratio (CMR).

Several researchers have conducted experimental and numerical investigations which indicates the numerous possibilities of utilizing SMAs in civil engineering structure. (Youssef et al. 2008) designed and tested two large scale beam-column joint sub-assemblages (referred as BCJ subsequently), one with SMA in the plastic hinge zone of the beam and other with regular steel rebar. They concluded that SMA-RC BCJ was able to recover the post-yield deformation while requiring minimum amount of repair compared to the steel-RC counterpart. (Billah and Alam 2012) conducted a numerical investigation on a hybrid SMA-FRP column with SMA bars at the plastic hinge regions and concluded that columns reinforced with SMA in the plastic hinge region reduced the residual drift considerably while showing good energy dissipation capacity. (Alam et al. 2009) numerically investigated the performance of concrete frame structures reinforced with superelastic SMA in the plastic hinge region of the beam and regular steel in other areas of the frame. Their results show that SMA-RC joints performed better in terms of recovering post-elastic rotations. (Elbahy et al. 2018) investigated the seismic performance of a retrofitted moment resisting frame using external SMA rebars. They concluded that the frame retrofitted using external SMA rebar sustained lower level of damage at the same earthquake intensity as compared to the steel counterpart.

Most of the research to date has focused on Ni-Ti SMA rebar, commonly known as Nitinol. Research addressing the application and seismic performance assessment of different types SMAs in concrete beam-column joint is missing in the literature. However, before the practical application of SMA in beam-column joints, it is necessary to evaluate the seismic collapse safety of beam-column joints reinforced with SMA. This study aims to evaluate the seismic collapse performance of five different SMA-RC beam-column joints considering maximum drift as the demand parameter. This will allow to compare the seismic collapse capacity as well as provide insight on the influence of SMA type in designing RC connections with little damage and reducing the post-earthquake damage repair cost.

2 DESIGN AND GEOMETRY OF BEAM-COLUMN JOINT

This section briefly describes the SMA-RC beam-column joint used in the study. A residential seven storey building located in Dhaka, Bangladesh is considered here. The building is designed and detailed according to the Bangladesh National Building Code (BNBC-2016). The plan view of the building are shown in Figure 1 (a). The exterior beam-column joint is isolated from the building at the points of contra-flexure from the mid-height of the second floor to the mid-height of the third floor (joint A). Beam length is considered up to the mid-span of the bay. The storey height of the building is 3.44 m. The spacing of the column is 3.96 m and 4.67 m in horizontal and transverse directions, respectively as shown in Figure 1 (a). Figure 1 (b) shows the cross section of the beam-column joint. The cross-section of the column is 250 mm x 500 mm with 12-20 mm diameter longitudinal reinforcement. The spacing of the rectangular tie is 125 mm at the joint, up to a length of (±750 mm) from the face of the joint and in the remaining length of the column spacing is maintained as 150 mm. The cross-section of the beam is 250 mm x 400 mm. The longitudinal reinforcement is similar for all types of joints, except that SMA is used only in the plastic hinge region of the five SMA-RC joints.

Five different SMA rebars, as shown in Table 1 (Billah and Alam 2016), were used to design the beam-column joints. The beam-column joints are designated as SMA-RC-1 (reinforced with SMA-1), SMA-RC-2 (reinforced with SMA-2), SMA-RC-3 (reinforced with SMA-3), SMA-RC-4 (reinforced with SMA-4), SMA-RC-5 (reinforced with SMA-5). SMA-RC-1 is reinforced with 8-20 mm SMA-1 bars, SMA-RC-2 reinforced with 8-20 mm SMA-2 bars, SMA-RC-3 reinforced with 8-16 mm SMA-3 bars, SMA-RC-4 reinforced with 8-28 mm SMA-4 bars, and SMA-RC-5 reinforced with 8-24 mm SMA-5 bars. The sizes of the bars are selected in such a manner that the axial force developed on the bars is similar. SMA is used only in the

plastic hinge region of the beam, with the remainder of the beam is detailed with regular steel. The material properties used for steel and concrete beam-column joint are summarized in Table 2. In the SMA-RC beam-column joint SMA is used only in the plastic hinge region of the beam, with the remainder of the beam is detailed with regular steel. The plastic hinge region was calculated using Paulay and Priestley (1992) equation. As the diameter and yield strength is different for five different types of SMA hence the length of plastic hinge varies accordingly.

[1] $L_p = 0.08L + 0.022d_b f_y$

Where L = length of the member in mm; d_b= bar diameter in mm; and f_y = yield strength of the rebar in MPa

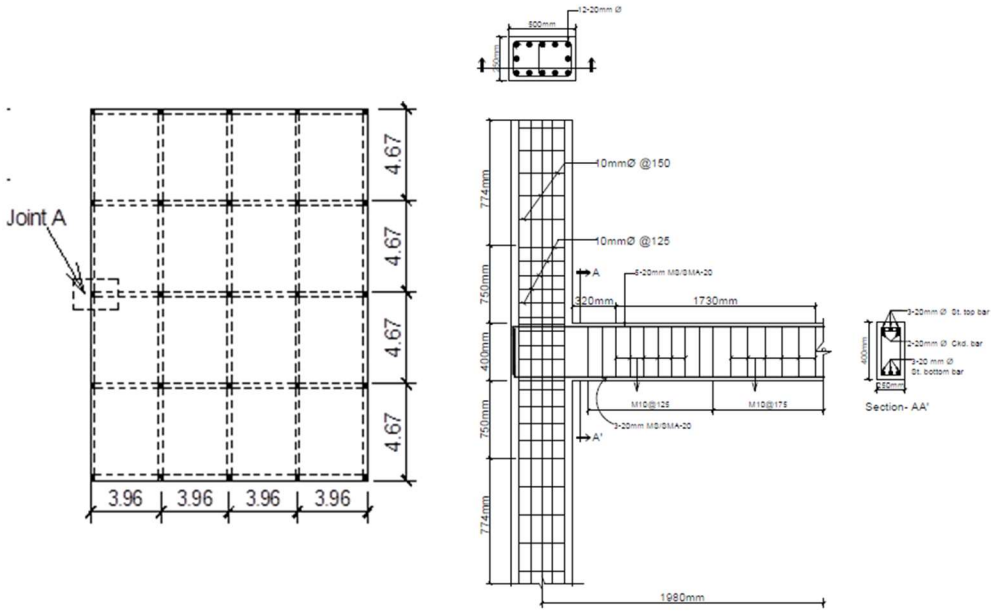

Figure 1: (a) Plan of a seven storey residential building (Dimension in meters) (b) Reinforcement detailing of beam-column joint

Table 1: Properties of different types of SMA

	Alloy	εs (%)	E (GPa)	f_Y (MPa)	f_{P1} (MPa)	f_{T1} (MPa)	f_{T2} (MPa)
SMA-1	$NiTi_{45}$	6	62.5	401.0	510	370	130
SMA-2	$NiTi_{45}$	8	68	435	535	335	170
SMA-3	FeNCATB	13.5	46.9	750	1,200	300	200
SMA-4	CuAlMn	9	28	210	275	200	150
SMA-5	FeMnAlNi	6.13	98.4	320	442.5	210.8	122

f_y (austenite to martensite starting stress); f_{P1} (austenite to martensite finishing stress); f_{T1} (Martensite to austenite starting stress); f_{T2} (martensite to austenite finishing stress); ε_s (superelastic plateau strain length); and E (modulus of elasticity)

3 Analytical Modelling of Beam-column joint

In this study, a fiber element based nonlinear analysis program SeismoStruct V7.0.4(Seismosoft, 2016) has been employed for modeling different SMA-RC beam-column joints. The elements used for the modeling of beam-column joint are 3D beam-column inelastic displacement based frame elements. All the material used for finite element modeling were in built in seismostruct V7.0.4. Concrete has been modeled

according to the confinement model proposed by (Mander et al. 1998). To represent reinforcing steel in the beam and column the model of (Menegotto–Pinto 1973) is used. SMA has been modeled according to the model proposed by (Auricchio and Sacco 1997). Each element is sub divided into 200 by 200 fiber element in the transverse direction. One of the longitudinal elements of beam represents the plastic hinge length of the beam. The axial load was applied at the top of the column is 1112 kN. Incremental dynamic analyses (IDA) have been performed to determine the collapse safety of the SMA-RC beam-column joint using 20 set of earthquake ground motions.

Table 2: Material properties used in FE program

Material	Property	Value
Confined Concrete	Compressive strength (MPa)	35
	Strain at peak stress	0.002
	Tensile strength (MPa)	3.5
	Modulus of elasticity (GPa)	28.2
Unconfined concrete	Compressive strength (MPa)	24
	Strain at peak stress	0.002
	Tensile strength	0
Steel	Yield strength (MPa)	410
	Strain hardening parameter	0.005
	Modulus of elasticity (GPa)	200

As seismostruct is a commercial software, validation of the program is necessary before starting the numerical model of SMA-RC beam column joint. Several researchers have demonstrated the accuracy of the program by validating the result found from experimental study (Alam et al. 2008, Billah and Alam 2013). An experimental study of SMA-RC beam-column joint conducted by (Youssef et al. 2008) has been used in this study for the validation of the program. Figure 3 show the comparison of the experimental result with the numerical modeling.

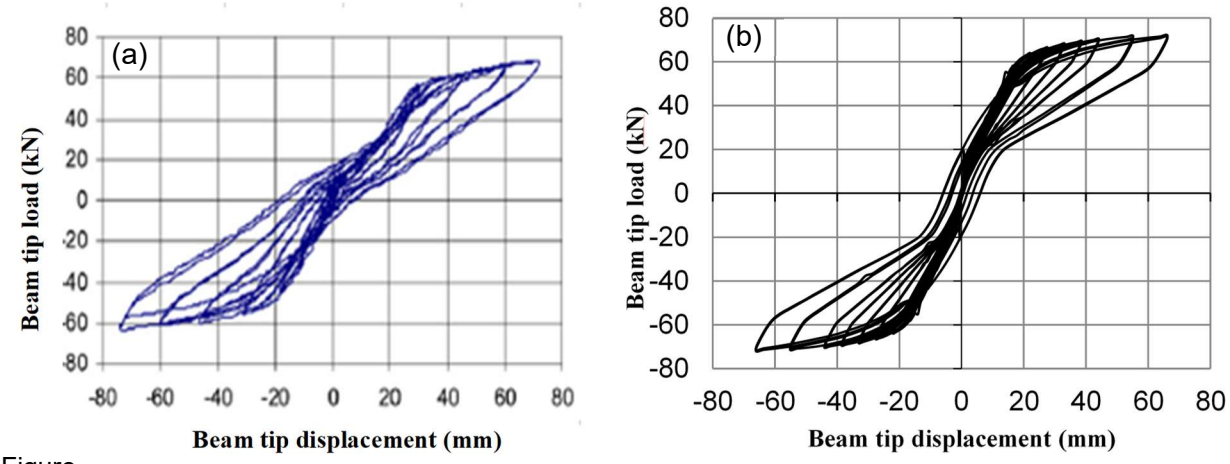

Figure 3 (a) Beam tip load versus beam tip displacement: (a) experimental result of SMA-RC joint Youssef et al. (2008) (b) Numerical result of SMA-RC joint

From the beam tip load versus displacement graph it is seen that ultimate beam tip load is found to be 70 kN at a beam tip displacement of 68 mm as shown in Figure 3 (b). Whereas from the experimental result the value of beam-tip load is 66.5 kN at the same tip displacement. The total energy dissipation capacity in numerical modeling is 5.5% higher than the experimental result.

4 PERFORMANCE ASSESSMENT APPROACH

IDA is a very useful method for evaluating the seismic performance of structures. In this process the structure is subjected to seismic excitation of different intensity levels. Each ground motion records is scaled (scaled up and/or down) to different intensity level while tracking the response of the structure in terms of displacements and acceleration etc. (Vamvatsikos, and Cornell 2002). Results from the incremental dynamic analysis have been used for the development of collapse fragility curves. In this study, the probabilistic seismic demand model (PSDM) has been used to derive the analytical fragility functions through incremental dynamic analysis of different beam-column joints. For this study, the cloud approach of PSDM has been used to develop the seismic fragility curve of the beam-column joints. This study developed fragility curves for different SMA-RC beam-column joint considering maximum drift as engineering demand parameter.

In the PSDM approach, the mean and standard deviation for different limit states were derived based on the power-law function which yields a logarithmic correlation between the engineering demand parameter and the selected intensity measure as shown below

[2] $EDP = a(IM)^b \; or, \ln(EDP) = \ln(a) + b\ln(IM)$

Here, a and b are unknown coefficients estimated through linear regression analysis of the damage state data obtained from the incremental dynamic analysis. The dispersion value for the demands $\beta_{EDP/IM}$ was estimated according to the equation below (Baker and Cronell 2006)

[3] $$\beta_{EDP|IM} = \sqrt{\frac{\sum_{i=1}^{N}\left(\ln(EDP) - \ln\left(aIM^b\right)\right)^2}{N-2}}$$

Where N is the total number of simulation cases.

Fragility curves for different damage states are generated using the following equation from Padgett (2007)

[4] $$P[DS \mid IM] = \phi\left[\frac{\ln(IM) - \ln(IM_n)}{\beta_{comp}}\right]$$

where Φ[ ] is the standard normal cumulative distribution function and

[5] $$\ln(IM_n) = \frac{\ln(S_c) - \ln(a)}{b}$$

IM_n is defined as the median value of the intensity measure for the selected damage states which are discussed in the next section. The dispersion component is presented in Equation 6.

[6] $$\beta_{comp} = \frac{\sqrt{\beta_{EDP|IM}^2 + \beta_c^2}}{b}$$

Here, (S_c) and (β_c) are the median and dispersion values for the damage states of the reinforced concrete buildings respectively.

Fragility provides a relationship between different engineering demand parameter (EDP) with respect to ground motion intensity measure (IM). Commonly used IMs in fragility analysis are Peak Ground acceleration (PGA), Peak Ground Velocity (PGV), and 5% damped Spectral Acceleration at the structure's first-mode period (Sa (T1,5%)). In this study, Sa (T1,5%) is considered as the IM since it is recommended by different guidelines (FEMA-P695) and researchers (Vamvatsikos and Cornell 2002, Shome et al. 1998).

4.1 Selection of Ground Motion

In this study, a total of 20 ground motions among which 10 near fault and 10 far field was considered for the incremental dynamic analysis. For this study, the near fault ground motions data were collected from the SAC steel project and the far field earthquake ground motions data were obtained from the Applied Technology Council far field ground motion set (ATC 1996). All these ground motions data were then matched with the acceleration response spectrum specified by Bangladesh National Building Code (BNBC 2016) for seismic site class SC. Table 3 and Table 4 presents different characteristics of the earthquake ground motions data for both the near fault and far filed earthquake motions considered in this study.

Table 3: Characteristics of far field ground motions

EQ No	Earthquake	Recording Station		Epicentral distance (km)	PGAmax (g)	PGVmax (cm/s.)
	M	Name				
FF1	6.7	Northridge	Beverly Hills	13.3	0.42	58.95
FF2	7.3	Landers	Yermo Fire	86	0.24	52
FF3	7.3	Landers	Coolwater	82.1	0.28	26
FF4	7.1	DuzceBolu	Bolu	41.3	0.73	56.44
FF5	6.9	Loma Prieta	Gilroy Array #3	31.4	0.56	36
FF6	6.5	ImpValley	El Centro Array#1	29.4	0.36	34.44
FF7	6.9	Kobe	Akashi	18.7	0.51	37.28
FF8	6.5	Super Hills	Poe Road	11.2	0.45	36
FF9	7.6	Chi-Chi	CHY	32	0.35	71
FF10	7.6	Chi-Chi	TCU	77.5	0.47	37

Table 4: Characteristics of near field ground motions

EQ No	Earthquake	Recording Station		Epicentral distance (km)	PGAmax (g)	PGVmax (cm/s.)
	M	Name				
NF1	7.4	Tabas	-	1.2	0.90	108
NF2	7.4	Tabas	-	1.2	0.96	103.8
NF3	7	Loma Prieta	Los Gatos	3.5	0.70	170
NF4	7	Loma Prieta	Lex. Dam	6.3	0.37	67.34
NF5	6.7	Erzincan	Erzincan	2	0.42	117
NF6	7.3	Landers	Lucrene Valley Stn.	1.1	0.79	69
NF7	6.7	Nothridge	Rinaldi	7.5	0.87	171
NF8	6.7	Nothridge	Olive View	6.4	0.72	120
NF9	6.9	Kobe	JMA	3.4	1.07	157
NF10	6.9	Kobe	Takatori	4.3	0.77	170.5

4.2 Probabilistic Seismic Demand Model

Incremental Dynamic Analyses (IDAs) are performed using the selected 20 earthquake records for the five different types of SMA-RC beam-column joints. The maximum drift found from IDA is considered as engineering demand parameter and spectral acceleration value at 5% damping ratio at the fundamental period of structure is considered as the intensity measure. A linear regression analysis is carried out between EDP and IM to estimate the value of a, b and dispersion demand $\beta_{EDP|IM.}$. The regression parameters along with the dispersion values obtained from the regression analysis are presented in Table 5

Table 5: Probabilistic seismic demand models for different joints in terms of maximum drift

Beam-column Joint Type	a	b	$\beta_{EDP\|IM}$
SMA-RC-1	2.41	2.13	1.81
SMA-RC-2	2.39	2.29	1.98
SMA-RC-3	2.36	2.26	1.95
SMA-RC-4	2.48	2.29	2.09
SMA-RC-5	2.53	2.36	2.06

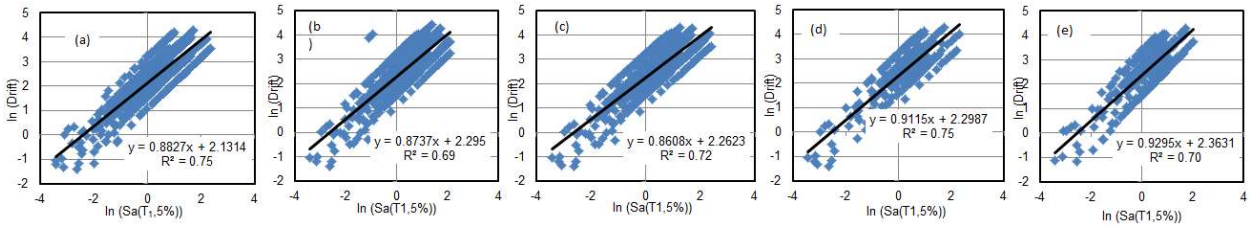

Figure 4: Comparison of the probabilistic seismic demand models for (a) SMA-RC-1 (b) SMA-RC-2 (c) SMA-RC-3 (d) SMA-RC-4 and (e) SMA-RC-5.

From the table it is evident that using Ni-Ti based SMA in the plastic hinge region of beam-column joint reduces the dispersion in demand compared other Cu based and Fe based SMA. The dispersion demand for SMA-RC-4 and SMA-RC-5 is 14% and 12% higher than SMA-RC-1 beam-column joint. On the other hand, SMA-RC-5 shows the greater median value of demand due to its higher elastic modulus and lower yield strength. It reveals that SMA-RC-3 are effective in reducing the maximum drift of the beam-column joint which is exhibited by a reduction in the parameters affecting both the coefficient (a) and (b) of the regression model.

Figure 4 shows the probabilistic seismic demand models for the five different SMA-RC beam-column joint considered for this study. Each figure depicts the corresponding linear regression equation and R^2 value. From Fig. 4, it is evident that all the PSDMs have a R^2 value higher that 0.7 which indicates a strong correlation between the considered EDP and IM.

4.3 Characterization of Damage States

(FEMA 2009) identified three permissible damage states to assess the seismic vulnerability of reinforced concrete building known as Immediate occupancy (IO), Life safety (LS), Collapse prevention (CP) damages with a transient drift limit of 1%, 2% and 4% respectively, at design level spectral acceleration. In this study, these damage states are quantified in terms of performance based limit states developed through pushover analysis for maximum drift (Nahar 2018). The median (S_c) used for the fragility analysis are shown in Table 6. The value of β_c is considered as 0.25 for immediate occupancy, for life safety this value is 0.30, whereas for collapse level damage this value is considered as 0.40 according to (FEMA-2009).

Table 6: Limit state capacity of steel and different types of SMA-RC beam-column joints

Damage State	Performance Criteria	SMA-RC-1	SMA-RC-2	SMA-RC-3	SMA-RC-4	SMA-RC-5
Immediate occupancy	*Sc*	0.90	0.90	0.90	0.90	0.90
Life safety	*Sc*	1.50	1.62	3.80	1.68	1.60
Collapse Prevention	*Sc*	3.00	3.06	3.35	2.94	3.06

4.4 Fragility Curve

Fragility curves for the five SMA-RC beam-column joints have been developed using the IDA results. Figure 5 shows the fragility curves for the five beam-column joint when maximum drift is considered as the EDP. Here the collapse fragility curve is developed for three damage states found from FEMA guideline. The evaluation of the fragility curves offered a valuable insight on the performance of different SMAs in reducing the probability of damage considering the maximum drift. From the figure it can be observed that the use of different types of SMA vary the probability of exceeding a certain damage states. At the immediate occupancy damage state, all five beam-column joints show similar behavior. The effect of different SMA is more pronounced on the life safety damage state. As depicted in Figure 5b, SMA-RC-5 is more likely to exceed life safety damage state at a lower intensity while SMA-RC-3 showed much better performance as it showed only 10% probability of exceeding life safety damage state at Sa (T1, 5%) of 0.6g. This can be attributed to the very high yield strength of SMA-3 as compared to other SMAs. However, an interesting behavior is observed in collapse prevention damage state where SMA-RC-3 has slightly reduced probability of exceedance as compared to life safety damage state. This can be attributed to the capacity limit states of life safety damage state considered in this study where SMA-RC-3 has higher drift limit before entering the life safety damage state as compared to collapse prevention state. However, in terms of probability of exceeding collapse prevention damage state, all five SMA-RC beam column joint showed comparable performance with less than 20% probability of exceedance at Sa (T1, 5%) of 0.6g.

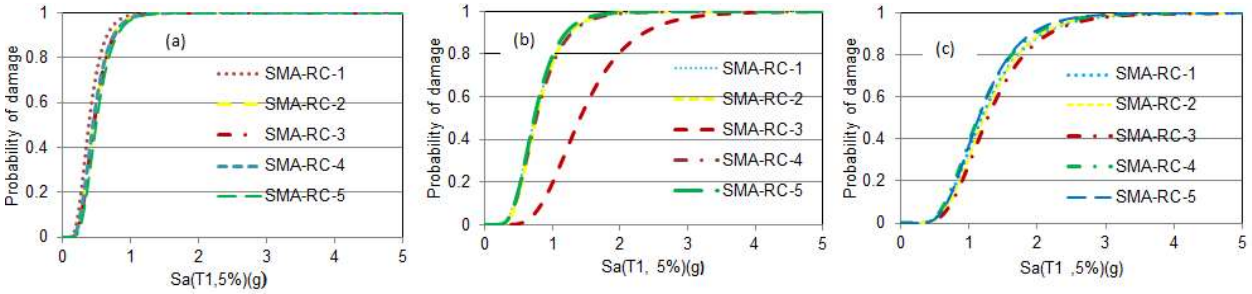

Figure 5: Fragility curves for the five beam-column joint (a) immediate occupancy (b) life safety (c) collapse prevention considering maximum drift.

4.5 Collapse Margin Ratio of Beam-Column Joint

Collapse margin ratio is defined as the ratio between the 5% damped spectral acceleration of the collapse level ground motion S_{CT} to the 5% damped spectral acceleration of maximum considered earthquake (MCE) ground motion, S_{MT} at the fundamental period of the seismic force resisting system of interest (FEMA 2009). The collapse fragility curve is used to determine the collapse margin ratios of the five SMA reinforced beam-column joints. However for CMR calculation only collapse based fragility curve is considered. Figure 6 median collapse level intensity (SCT) at which 50% of the ground motions cause the beam-column joint to collapse.

Table 7 shows the summary of the calculated results in terms of maximum demand parameter. The increase in collapse margin ratio indicates an overall increase of the collapse capacity of the building. From the table it is observed that higher collapse margin ratio is found for SMA-RC-3 beam-column joint which is almost

11% higher than regular SMA-RC-5 beam-column joint. Collapse margin ratio of other SMA-RC beam column joint is almost comparable to SMA-RC-3 beam-column joint. Smaller elastic modulus of SMA-RC-4 results the lowest collapse margin ratio among other types of SMA which is 5.53% lower than SMA-RC-1, 8.15% lower than SMA-RC-2, 11% lower than SMA-RC-3 beam column joint.

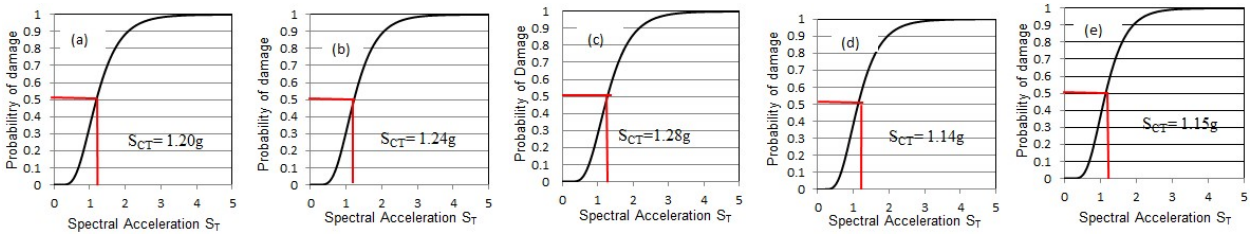

Figure 6: Collapse fragility curve for (a) SMA-RC-1 (b) SMA-RC-2 (c) SMA-RC-3 (d) SMA-RC-4 and (e) SMA-RC-5 beam-column joint in terms of maximum drift.

Table 7: CMR for different beam-column joints in terms of maximum drift

	SMA-RC-1	SMA-RC-2	SMA-RC-3	SMA-RC-4	SMA-RC-5
Median Collapse Level, $S_{CT(g)}$	1.20	1.24	1.28	1.14	1.15
MCE Demand, $S_{MT(g)}$	1.01	1.01	1.01	1.01	1.01
Collapse Margin Ratio (CMR)	1.18	1.22	1.27	1.13	1.13

5 CONCLUSION

In this study, the performance of five different SMA reinforced beam-column joints has been investigated in terms of fragility curves and Collapse Margin Ratio (CMR) using twenty set of earthquake ground motions. For reinforcing the beam-column joints, two Ni-Ti based, one Cu-based, and two Fe-based SMAs are used in the plastic hinge region of beam-column joints. Based on the analysis of the results, the following conclusions can be drawn:

1. Among two Ni-Ti based SMA, SMA-RC-1 show 4% higher probability of collapse than SMA-RC-2 beam-column joint.
2. The safety against collapse for SMA-RC-3 beam column joint is almost 4% to 11% higher than other SMA-RC beam-column joints in terms of maximum drift as the demand parameter.
3. At spectral acceleration at the fundamental period of the structure, the probability of damage for SMA-RC-3 beam-column joint is 12% higher at the collapse prevention condition (Damage state 3) than the life safety condition (Damage state 2) due to high yield strength of the Fe based SMA-RC-3.
4. The engineering demand parameter and intensity measure considered in this study are the maximum drift and spectral acceleration at the fundamental time period of the structure. Result of the regression analysis indicates the better correlation between these two parameters.

6 REFERENCES

Applied Technology Council, ATC-40. 1996. Seismic Evaluation and Retrofit of Concrete Buildings, California, Volumes. 1 and 2.

Auricchio, F., and Sacco, E., 1997. Superelastic Shape-Memory-Alloy Beam Model. *Journal of Intelligent Material Systems and Structures*, **8** (6): 489–501.

Alam, M., Youssef, M., and Nehdi, M. 2008. Analytical Prediction of the Seismic Behaviour of Superelastic Shape Memory Alloy Reinforced Concrete Elements. *Engineering Structures*, **30** (12): 3399-3411.

Alam, M.S., Youssef, M.A., and Nehdi, M. 2009. Seismic Performance of Concrete Frame Structures Reinforced with Superelastic Shape Memory Alloys. *Smart Structure and System,* **5**(5): 565-585.S

Baker, J.W. and Cornell, C.A. 2006. Vector-valued ground motion intensity measures for probabilistic seismic demand analysis. *Pacific Earthquake Engineering Research report*, PEER Center, University of California Berkeley, 2006/08

Bangladesh National Building Code. 2016. Housing and Building Research Institute, Bangladesh Standard and Testing Institute.

Billah A.H.M.M., Alam M.S. 2012. Seismic Performance of Concrete Columns Reinforced with Hybrid Shape Memory Alloy (SMA) and Fiber Reinforced Polymer (FRP) Bars. *Construction and Building Material*, **28**(1): 730–42.

Billah, A.H.M.M., Alam, M.S. and Bhuiyan, A.R. 2013. Fragility Analysis of Retrofitted Multi-column Bridge bent Subjected to Near Fault and Far field Ground Motion. *ASCE Journal of Bridge Engineering,* **18** (10): 992-1004

Billah, A.H.M.M.and Alam, M.S. 2016. Performance-based Seismic Design of Shape Memory Alloy–Reinforced Concrete Bridge Piers. I: Development of Performance-based Damage States. *Journal of Structural Engineering*, **142** (12): 04016140.

Clark P. W., Aiken I., Kelly J. M., Higashinho M. 1995. Experimental and Analytical Studies of Shape Memory Alloy Dampers for Structural Control. *Earthquake Engineering Research Center* 1301 South 46th Street, University of California at Berkeley, Richmond, California 94804, *SPIE* **2445**: 241-251

Elbahy, Y.I., Youssef, M.A., Meshaly, M. 2018. Seismic Performance of Reinforced Concrete Frames Retrofitted Using External Superelastic Shape Memory Alloy Bars. *Bulletin of Earthquake Engineering*, 1-22.

FEMA P695. 2009. Quantification of Building Seismic Performance Factors. Federal Emergency Management Agency, Washington DC

Mander, J.B., Priestley, M.J.N. and Park, R. 1988. Theoretical Stress–strain Model for Confined Concrete. *Journal of Structural Engineering*, **114** (8): 1804–26.

Menegotto, M., and Pinto, P.E. 1973. Method of Analysis for Cyclically loaded R.C. Plane Frames including Changes in Geometry and non-elastic Behaviour of Elements under Combined normal Force and Bending. *Symposium on the Resistance and Ultimate Deformability of Structures Acted on by Well Defined Repeated Loads*. International Association for Bridge and Structural Engineering, Zurich, Switzerland, 15-22

Nahar, M. 2018. Seismic Collapse Safety Assessment of RC Beam-column Joint Reinforced with different types of Shape Memory Alloy Rebar. *M.Sc Thesis*, Military Institute of Science and Technology, Dhaka

Paulay, T., Priestley, M.N.J. 1992. Seismic Design of Reinforced Concrete and Masonry Buildings. New York, NY: John Wiley & Sons, Inc

Padgett, J.E. 2007. Seismic vulnerability assessment of retrofitted bridges using probabilistic methods. *PhD Thesis*, Georgia Institute of Technology, Atlanta.

Ramirez, C. M., Miranda, E.2012. Significance of Residual Drifts in Building Earthquake Loss Estimation. *Earthquake Engineering & Structural Dynamics*, **41** (11): 1477–1493.

Shome, N., Cornell, C.A., Bazzurro, P., and Carballo, J. E., 1998. Earthquakes, records, and Nonlinear Responses. *Earthquake Spectra*, **14** (3): 8755–2930.

SeismoSoft, 2016. SeismoStruct - A computer program for static and dynamic nonlinear analysis of framed structures, V 7.0.4 [online], available from URL: www.seismosoft.com.

USGS Real-time Earthquake Map with Exact dates and live Earthquake Reports. United States Geological Survey.

Vamvatsikos, D., & Cornell, C. A., 2002. Incremental Dynamic Analysis. *Earthquake Engineering & Structural Dynamics*, **31** (3):491–514

Youssef, M.A., Alam, M.S., Nehdi, M. 2008. Experimental Investigation on the Seismic Behavior of Beam–column joints reinforced with Superelastic shape memory alloys. Journal of Earthquake Engineering, **12** (7): 1205–1222.